Stress Prediction Using Machine Learning and Optimization

G. Mahalakshmi
Department of Computer Science, Sri Meenakshi Government Arts College for Women, Affiliated to Madurai Kamaraj University, Madurai, India
gmahalakshmiphd2021@gmail.com (corresponding author)

G. Sujatha
Department of Computer Science, Sri Meenakshi Government Arts College for Women, Affiliated to Madurai Kamaraj University, Madurai, India
sujisekar05@gmail.com

Nisha Jebaseeli Antony
Department of Computer Science, CDOE-Bharathidasan University, Tiruchirappalli, India
antonycruznisha@gmail.com

A. Bhuvaneshwari
Department of Computer Science and Applications, SRM Institute of Science and Technology, Ramapuram, Chennai, India
bhuvanea1@srmist.edu.in

S. Vasuki
Department of Computer Science, Srivanchi College of Arts and Science, Sathyamangalam, Pudukkottai, India
vasukisankarjothi1980@gmail.com

Received: 28 December 2025 | Revised: 27 January 2026, 14 February 2026, and 27 February 2026 | Accepted: 28 February 2026

 DOI: https://doi.org/10.48084/etasr.17218

ABSTRACT

Conventional stress prediction methods have high computational cost and poor generalization and noise sensitivity, which can limit their application in real-time. To address these challenges, this study presents an integrated framework that combines signal preprocessing, lightweight feature extraction, segmentation, classification, and adaptive optimization. Ultrasonic Guided Wave (UGW) signals are first processed using a Butterworth filter to suppress noise and enhance signal quality. The features are then extracted through Tiny Machine Learning (TinyML), enabling efficient deployment on resource-constrained devices. For segmentation, a Multi-Scale Attention Augmented U-Net (MA-U-Net) is employed to capture stress fields across multiple resolutions while focusing on critical regions. Classification of damage states is performed using a Multilayer Perceptron (MLP), which effectively models nonlinear interactions. Finally, an Adaptive Stress-Strain Optimization Strategy (ASSOS) refines the model parameters under physics-based constraints to ensure robust convergence. The framework was validated on the Open Guided Wave dataset, achieving 98.75% accuracy, with precision, recall, and F1 scores exceeding 98%. Comparative analysis confirmed superior performance over conventional FEM and Random Forest models. This unified approach offers a scalable solution for structural health monitoring. This proposed framework is a combined scheme, very precise and efficient in the prediction of the stress, offering scalable structural health monitoring.

Keywords-machine learning; Butterworth filter; stress prediction; multilayer perceptron; Adaptive Stress Strain Optimization Strategy (ASSOS)

I. INTRODUCTION

Structural Health Monitoring (SHM) is an essential part of maintaining the integrity of composite structures, especially in high-risk applications such as aerospace and civil engineering, where undiscovered stress/damage can cause catastrophic failure [1, 2]. Multimodal fusion approaches that include physiological, behavioral, and contextual data show promise in improving robustness [3-8]. Few studies were designed to combine the above elements with Ultrasonic Guided Waves (UGW) signals, attention mechanisms for feature extraction in spatial-temporal domains, on-device lightweight processing, and adaptive optimization to focus on the nonlinear behaviors of materials and environmental noise.

Recent developments in TinyML allow low-power, edge-based inference for physiological or acoustics monitoring [9-11]. Other systems have serious limitations, especially regarding memory, processing power, and model complexity, and their limited ability to deploy it in resource-constrained SHM use cases with real-time requirements [12] Physics-based approaches, such as the Finite Element Method (FEM), often become difficult for complex non-linear geometrical structures, dynamic loading conditions, having high computation requirements and long analysis times [13, 14]. Machine learning approaches, such as Multilayer Perceptron (MLP) for non-linear mapping [15-18], and Ultrasonic Guided Waves (UGW) have become an exciting non-destructive approach for detecting anomalies over large areas with a minimum number of sensors with a high sensitivity to detect early-stage damage in Carbon Fiber-Reinforced Polymer (CFRP) plates [19-22]. The Open Guided Waves (OGW) platform [23] consists of valuable open-access benchmark datasets for UGW propagation in controlled CFRP setups to reproducibly validate detection methods.

This study overcomes these key shortcomings and proposes an integrated and scalable framework for stress prediction that connects physics-based modeling and data-driven techniques. The approach involves the application of the Butterworth filtering algorithm for noise-robust preprocessing of UGW signals, TinyML optimized feature extraction to optimize edge efficiency, a Multi-scale Attention augmented U-Net (MA-U-Net) for accurate stress field segmentation, an MLP classifier to model complex nonlinear interactions, and an Adaptive Stress-Strain Optimization Strategy (ASSOS) to optimize brittle new parameter optimization and convergence driven by the physical constraints.

II. PROPOSED METHOD

This study provides a universal method for predicting stress using a Butterworth filter to preprocess ECG signals by eliminating high-frequency noise, thus enhancing signal quality to make a correct judgment of stress levels. The MA-U-Net model predicts the structural stress fields using both multi-scale convolution kernels and an attention mechanism, which enhances the efficiency and accuracy of the prediction. ASSOS is an iterative stress and strain optimization scheme that utilizes error minimization algorithms, mesh segmentation, and scaling of models to optimize the Adaptive Stress and Strain Prediction Model (SSAPM). This results in the correct modeling of complicated material behavior and high computational efficiency. OGW provided experimental data to improve the validity and accuracy of the stress prediction models in the structural-based health monitoring frameworks to model and analyze the dynamics of the UGWs in a carbon fiber composite plate. Figure 1 shows the proposed architecture workflow.

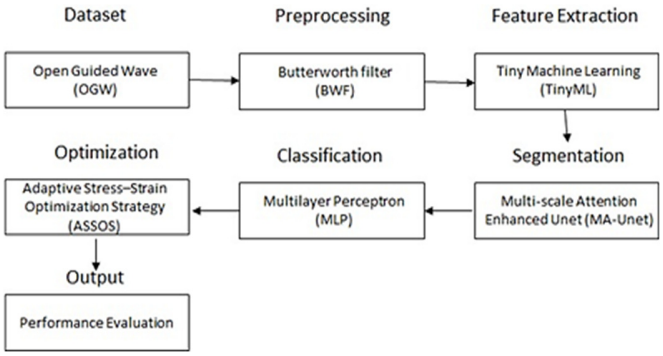

Fig. 1. Proposed workflow.

A. Dataset

OGW is an open-access online dataset consisting of UGW data from 12 sensors on a 0.5×0.5 m carbon fiber-reinforced polymer plate. The aluminum disk used to simulate plate damage was 10 mm in diameter, 2.35 mm high, and had a mass of 0.5 g. The disk interacted with the UWI sound waves transmitted through the transducer. In this paper, any change in the signal is noted as a "damage." The Handyscope HS5 was used to create an arbitrary waveform and acquire the signal using a 14-bit analog-to-digital converter. The PD200 wideband amplifier (piezoelectric driver) amplifies the signal. The excitation waveform is selected with a dedicated multiplier route to the signal from an amplifier. This establishes controls of motor and receiver pairs using TDM and records signals in HDF5 format. Measurements were performed in a climate chamber to reduce the effect of environmental influences.

B. Preprocessing Butterworth Filter (BWF)

By applying BWF, an average of the baseline measurements was obtained by the filter response through the passband up to the –3 dB cutoff frequency, giving a –20 dB per decade decay at the stopband. The tests carried out in a climate chamber under identical conditions had all 60 baselines in one master baseline for all types of damage. The same strategy makes the model sensitive to subtle changes and was repeated for all sweeps of the transducer frequency. This resulted in the production of 66 baselines per frequency, although only 40 kHz of data was used in the final model. Table I provides technical details on the Butterworth filter.

C. Feature Extraction-Tiny Machine Learning (Tiny ML)

The process transforms raw physiological measurements into a defined set of meaningful features to reduce the useless complexity. Tiny ML models are designed with low latency and low power, making them perfect for real-time stress prediction. Tiny ML allows for smart decisions at the edge, enabling stress prediction models to function very well in embedded systems. Table II shows feature extraction details.

TABLE I. BUTTERWORTH FILTER PARAMETERS

Parameter	Value/setting	Description
Filter type	Low-pass (or band-pass)	To remove high-frequency noise in UGW signals
Order	4th or 6th order	Chosen for sharp roll-off without excessive phase distortion
Cut-off frequency	200 kHz	Above max excitation (260 kHz) + margin
Passband ripple	<1dB	Flat response in the band of interest
Stopband attenuation	≥ 40 dB	Effective noise suppression
Implementation	Zero-phase (filtfilt in MATLAB/Python)	Avoid phase shift in time series
Baseline averaging	60 baselines averaged per frequency	Master baseline for damage-sensitive subtraction

TABLE II. TINY ML FEATURE EXTRACTION DETAILS

Component	Details	Value
Framework/ Library	TensorFlow Lite Micro / Edge Impulse	Microcontroller deployment
Extracted features	RMS, Peak amplitude, FFT peaks (top 5), wavelet coeffs (db4, level 3)	Handcrafted + learned embeddings
Model type	Small CNN or MLP	Post-quantization size < 200 KB
Input window	1024 samples	Sliding window on UGW time-series
Quantization	8-bit integer	Low-power inference

D. Segmentation - Multi-Scale Convolutional Neural Network (MA-U-NET)

This study developed the MA-U-Net to estimate voltage fields. The attention mechanism significantly enhanced the modeling capacity of the model by focusing on areas with essential features. These focal points help reduce external information during the feature extraction process, leading to higher accuracy and stability. Multi-scale convolution kernels were proposed to extract features from different scales. MA-U-Net can acquire stress fields and the evolution of the structural features for multi-scale convolution kernels, which learn features at different scales from filters of different sizes, from specifics to larger patterns. Table III presents the parameters of the MA-U-NET architecture.

TABLE III. MA-U-NET ARCHITECTURE PARAMETERS

Layer/block	Kernels size/Filters	Activation
Encoder level 1	1×1, 2×2, 3×3 conv stacks	RELU
Encoder level 2	64 filters	RELU
Encoder level 3	128 filters	RELU
Attention mechanism	Channel/Spatial	-
Decoder upsampling	Transposed conv 2×2	RELU
Loss function	Dice+Binary Cross-Entropy	Scheduler: Reduce LR OnPlateau
Optimizer/LR	Adam / 1e-3 initial	Early stopping
Batch size/Epochs	16/200	Early stopping on val loss

Figure 2 shows the multi-scale convolution stack layout. The input image has different dimensions. Each kernel size undergoes two convolutions, and then the feature extraction results are combined. To focus on essential model regions, a self-tracking layer is added after the first and last hidden layers, then downsampled through max pooling to reduce feature map size while preserving spatial information. The encoder has three layers with 32, 64, and 128 kernels.

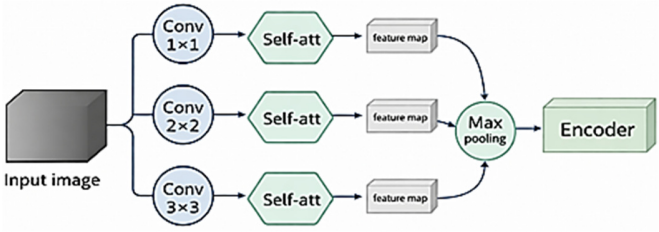

Fig. 2. MA-UNet Architecture.

E. Classification - Multilayer Perceptron (MLP)

MLP is a feed-forward neural network classifier based on backpropagation for learning maps and second-category classified examples. The transfer function is used to find the weighted input in each of the outputs of the neuron. Three measures were used to assess the model performance: Mean Absolute Error (MAE), Mean Absolute Percentage Error (MAPE), and coefficient of determination (R^2).

$$MAE = \frac{1}{n}\sum_{i=1}^{n}|y_i - y_1| \quad (1)$$

$$MAPE = \frac{100\%}{n}\sum_{i=1}^{n}\left|\frac{y_i - y_1}{y_i}\right| \quad (2)$$

$$R^2\,(y) = 1 - \frac{\sum_{i=1}^{n}(y_i - y_1)^2}{\sum_{i=1}^{n}(y_i - y_1)^2} \quad (3)$$

MAE is the difference between the predicted and real results, while MAPE determines the importance of the difference between the predicted and actual results. Together, these three indicators can determine the performance of the model quite comprehensively. Table IV shows the MLP parameters.

TABLE IV. MLP CLASSIFICATION PARAMETERS

Hyperparameter	Value	Setting
Hidden Layers	3	[2–5]
Neurons per layer	256 → 128 → 64	-
Activation	ReLU	-
Dropout rate	0.3	[0.1–0.5]
Optimizer	Adam	LR: 1e-3 to 1e-5
Batch size	32	-
Epochs	100	Early stopping

F. Adaptive Stress Strain Strategy(ASSOS)

ASSOS uses an iterative process to solve the problems of stress imbalance. It is responsible for ensuring steady progress towards a steady state of physical equilibrium. The gist of this method is to determine the residual error according to:

$$R = \nabla \cdot \sigma - f \quad (4)$$

$$\sigma_{n+1} = \sigma_n - \alpha\, R_n \quad (5)$$

The adaptive step size (a) is dynamically calculated using the linear mobility technique to optimize the minimization of R and stability. For the nonlinear physical behavior, this update uses a step-by-step approach.

$$\nabla\sigma = C : \Delta\varepsilon \quad (6)$$

Here, $\nabla\sigma$ and $\Delta\varepsilon$ are increments of stress and strain, while C is the tangential stiffness tensor for the material response. These types can describe phenomena such as plastic deformation and viscoelasticity creep, which represent path dependence.

Principles of energy are used to increase the stability and convergence; the total potential energy of the system is minimized at each step as:

$$\varepsilon = \int (\frac{1}{2}\sigma : \varepsilon - f \cdot u)\, d \quad (7)$$

where ε is the strain tensor, u is the displacement vector, and the energy gradient symbols are:

$$\Delta\varepsilon = \frac{\delta\varepsilon}{\delta\sigma} : \Delta\sigma \quad (8)$$

In addition, ASSOS applies adaptive relaxation techniques in regions of large gradients, which may result in fast variations of the stress and block convergence. A relaxation factor, which is represented by b, is introduced as:

$$\sigma_{n+1} = \sigma_n - \beta\alpha R_n \quad (9)$$

where $\beta \in (0,1]$ serves to adjust the correction magnitude. This is crucial for achieving stable convergence in complex situations, such as those occurring at crack tips or near phase boundaries. The dual residual criterion was used to ensure and verify convergence. The primary criterion is the residual stress criterion, which must be reduced to below a predetermined acceptable error level:

$$\|R\| < \varepsilon \quad (10)$$

The stress change between iterations of the second force satisfies:

$$\|\sigma_{n+1} - \sigma_n\| < \delta \quad (11)$$

where ε and δ are user-defined thresholds. Table V describes the ASSOS optimization strategy.

TABLE V. ASSOS OPTIMIZATION STRATEGY

Parameter	Value	Description
Initial step size (α)	0.1	Dynamically adapted via line search
Residual threshold (ε)	1e-6	Dynamically adapted via line search.
Relaxation factor (β)	0.8 (adaptive in high-gradient regions)	Stress equilibrium convergence
Max iterations	500	Stabilization near singularities

G. Dataset

This study utilized publicly available benchmarks from the OGW platform [23]. The dataset consists of UGW measurements on a quasi-isotropic Carbon Fiber-Reinforced Polymer (CFRP) plate of size 0.5 m × 0.5 m × 2 mm. Twelve piezoelectric transducers are distributed in two rows, with each six representing 66 unique pitch catch paths (transducer pairs) per measurement.

A total of 60 baseline measurements were taken under pristine conditions (20 measurements per day over three days) in a climate chamber at a constant temperature of 23°C and 50% relative humidity to minimize environmental variability. Damage was simulated with a 10 mm diameter, 2.35 mm high Al (with a mass of 0.5 g) disc placed in 28 different locations on the surface of the plate. Excitation frequencies varied from 40 kHz to 260 kHz in 20 kHz increments, and signals were measured using a Handyscope HS5 oscilloscope with a 14-bit ADC and stored as HDF5 files using a PD200 amplifier. Each of these signals lasts 1.31 ms or so.

H. Training and Evaluation Protocol

The whole set of processed instances (obtained from the 5808 signals) was randomly split into training (70%), validation (15%), and test (15%) sets. Stratification was used to ensure that the ratio of pristine-to-damaged samples is balanced in splits to avoid data leakage by ensuring whole damaged locations or transducer pairs were not split across sets. Training was performed with the maximum number of epochs as 200 for MA-U-Net (optimizer Adam, initial learning rate 1×10^{-3}, batch size 16) and 100 epochs for MLP (batch size 32), using early stopping when there was no improvement of the validation loss for 15 epochs (delta < 0.001) (MSE for regression tasks, cross entropy for classification). ASSOS optimization was limited to 500 iterations per instance (or to stress change < 1×10^{-4} and R < 1×10^{-6}). Final performance metrics (accuracy, precision, recall, and F1-score) were calculated on the held-out test set only to obtain unbiased results.

I. Implementation

The proposed model was implemented using Python Tensorflow for neural network processing, MATLAB for signal processing, and a piezoelectric transducer on a carbon fiber composite plate to generate UGWs. These waves travel on the plate and interact with the simulated damage. Twelve sensors were divided into just locations on the plate. The excitation frequency was between 40 and 260 kHz in 20 kHz increments.

III. RESULTS AND DISCUSSION

The 98.75% classification accuracy with ASSOS and its ability to exceed baselines by 1-2%, e.g., 96.38% SMO and ~97% PSO/GWO, was equivalent to substantially fewer undetected damages of CFRP structures. This is critical for safety in aerospace structures where even marginal improvements can prevent catastrophic failures under high-cycle fatigue operation. The narrow error band in MLP predictions (0.00-0.25 vs. RF up to 5.60) offers a higher reliability under different working conditions because the adaptive ASSOS updates (according to dynamic a and relief b) are more effective in mitigating residual imbalances in the nonlinear interactions between waves and wave damage compared to static optimizers. Compared to previous guided wave ML studies on OGW or equivalent data sets (95-97%) by CNN localization approaches, the superior 98.75% obtained by the proposed framework is due to the multi-scale attention segmentation given to multi-resolution damage features in the framework. ASSOS guarantees physics-constrained convergence. Unlike models with generalization problems, this is an extension of multimodal robustness to structural applications.

The proposed approach was evaluated using a confusion matrix and metrics such as accuracy, precision, recall, and F1 score.

$$\text{ACC} = \frac{\text{TP+TN}}{\text{TN+TP+FP+FN}} \quad (12)$$

$$\text{Precision} = \frac{\text{TP}}{\text{TP+ FP}} \quad (13)$$

$$\text{Recall} = \frac{\text{TP}}{\text{TP+FN}} \quad (14)$$

$$\text{F1} - \text{score} = 2 * \frac{\text{Precision*Recall}}{\text{Precision+Recall}} \quad (15)$$

Unlike traditional FEM-based approaches, which cannot deal with nonlinear geometries and require large amounts of computational resources, the proposed model realizes efficient computation while showing high sensitivity to slight stress variations. The combination of ASSOS also makes the proposed approach unique because optimization strategies can ensure convergence and accuracy even for complex material behaviors when other optimization strategies cannot maintain stability. In addition, the use of Tiny ML makes it possible to predict the stress in real-time on resource-constrained devices, which is not possible with the cloud-dependent or heavy-computing models. This makes the proposed approach not only more accurate but also practical when deploying systems in embedded and edge computing environments.

TABLE VI. CLASSIFICATION COMPARISON PERFORMANCE FOR OGW DATASET

Methods	Accuracy(%)	Precision(%)	Recall(%)	F1 score(%)	Specificity(%)
SMO	96.38	98.30	97.90	97.05	97.38
DBO	96.03	97.27	98.42	98.56	98.78
PSO	97.27	97.05	98.56	98.67	98.59
GWO	98.12	98.36	98.76	98.70	98.92
ASSOS (proposed)	98.75	98.84	98.88	98.85	98.02

SMO: Sequential Minimal Optimization, DBO: Dung Beetle Optimization, PSO: Particle Swarm Optimization
GWO: Gray Wolf Optimization, ASSOS: Adaptive Stress–Strain Optimization Strategy

IV. CONCLUSION

The proposed hybrid approach directly addresses an important knowledge gap identified in existing literature: there are still no scalable, noise-robust, real-time solutions that efficiently combine computationally expensive physics-based modeling (e.g., FEM) with data-driven approaches while retaining high accuracy and edge deployability. Achieving a classification accuracy of 98.75% with near-perfect precision, recall, and F1 scores on the OGW benchmark demonstrates the capabilities of adaptive physics-informed optimization and attention-guided feature focus to enhance the capabilities of traditional optimization algorithms and standalone ML models for handling nonlinear wave damage patterns.

Scientifically, this work validates the value of the multi-scale attention mechanism for environmental noise suppression and multi-resolution damage signature in guided waves, and, practically, low-power, real-time structural health monitoring on resource-constrained devices has direct relevance to aerospace applications for fatigue detection, damage detection on composite structures, and possible extension to multimodal stress monitoring in biomedical applications.

Despite these advances, there are still limitations, such as increased computational demands when models are scaled to larger or anisotropic structures and a lack of formal quantification of uncertainty, as well as bounding in terms of testing under actual operational variability (i.e., temperature gradients and vibration). To deal with these, future studies will (i) integrate Bayesian/ensemble uncertainty estimation into ASSOS for delivering probabilistic damage predictions and (ii) validate the framework using anisotropic composite samples and in-service environmental conditions.

REFERENCES

[1] M. Tanveer, M. U. Elahi, J. Jung, M. M. Azad, S. Khalid, and H. S. Kim, "Recent Advancements in Guided Ultrasonic Waves for Structural Health Monitoring of Composite Structures," *Applied Sciences*, vol. 14, no. 23, Nov. 2024, Art. no. 11091, https://doi.org/10.3390/app142311091.

[2] J. Heimann, S. Mustapha, B. Yilmaz, and J. Prager, "Guided Waves in Composite Overwrapped Pressure Vessels and Considerations for Sensor Placement Toward Structural Health Monitoring—An Experimental Study," *Journal of Nondestructive Evaluation, Diagnostics and Prognostics of Engineering Systems*, vol. 8, no. 3, Aug. 2025, Art. no. 031007, https://doi.org/10.1115/1.4067667.

[3] X. Sui, "Structural Health Monitoring Technology: Advances in Multi-Modal Sensing and Data Fusion," in *Proceedings of the 2025 2nd International Conference on Electrical Engineering and Intelligent Control (EEIC 2025)*, vol. 279, A. J. Moshayedi, Ed. Atlantis Press International BV, 2025, pp. 924–941.

[4] K. Luo, C. Li, H. Zhang, and Y. Zhang, "Baseline-free multimodal damage detection framework for composite plate-like structures using Mamba with guided waves," *Measurement*, vol. 257, Jan. 2026, Art. no. 118958, https://doi.org/10.1016/j.measurement.2025.118958.

[5] H. Lu, S. C. Chinchilla, B. Rotsaert, A. Croxford, K. Gryllias, and D. Chronopoulos, "Damage identification using ultrasonic Lamb waves with multi-scale adaptive attention Transformer-based unsupervised domain adaptation," *Mechanical Systems and Signal Processing*, vol. 234, July 2025, Art. no. 112772, https://doi.org/10.1016/j.ymssp.2025.112772.

[6] A. Elhanashi, P. Dini, S. Saponara, and Q. Zheng, "Advancements in TinyML: Applications, Limitations, and Impact on IoT Devices," *Electronics*, vol. 13, no. 17, Sept. 2024, https://doi.org/10.3390/electronics13173562.

[7] M. Maurizi, C. Gao, and F. Berto, "Predicting stress, strain and deformation fields in materials and structures with graph neural networks," *Scientific Reports*, vol. 12, no. 1, Dec. 2022, Art. no. 21834, https://doi.org/10.1038/s41598-022-26424-3.

[8] M. Y. Takara and K. A. Flanigan, "A Multimodal Fusion Architecture and Dataset: Advancing Camera and Geophone Integration for Smarter Infrastructure," in *Structural Health Monitoring 2025*, 2025, https://doi.org/10.12783/shm2025/37371.

[9] J. T. Hancock, T. M. Khoshgoftaar, and J. M. Johnson, "Evaluating classifier performance with highly imbalanced Big Data," *Journal of Big Data*, vol. 10, no. 1, Apr. 2023, Art. no. 42, https://doi.org/10.1186/s40537-023-00724-5.

[10] M. S. Khan *et al.*, "Comparison of multiclass classification techniques using dry bean dataset," *International Journal of Cognitive Computing in Engineering*, vol. 4, pp. 6–20, June 2023, https://doi.org/10.1016/j.ijcce.2023.01.002.

[11] L. Pan *et al.*, "An ultra-sensitive resistive pressure sensor based on hollow-sphere microstructure induced elasticity in conducting polymer film," *Nature Communications*, vol. 5, no. 1, Jan. 2014, Art. no. 3002, https://doi.org/10.1038/ncomms4002.

[12] L. Maio, V. Memmolo, N. Christophel, S. Kohl, and J. Moll, "Electromechanical admittance method to monitor ice accretion on a composite plate," *Measurement*, vol. 220, Oct. 2023, Art. no. 113290, https://doi.org/10.1016/j.measurement.2023.113290.

[13] S. Yu *et al.*, "Advancing spacecraft safety and longevity: A review of guided waves-based structural health monitoring," *Reliability Engineering & System Safety*, vol. 254, Feb. 2025, Art. no. 110586, https://doi.org/10.1016/j.ress.2024.110586.

[14] C. D. Coman, D. E. Crunteanu, G. Cican, and M. Stoia-Djeska, "Geometry Effects on Joint Strength and Failure Modes of Hybrid Aluminum-Composite Countersunk bolted Joints," *Engineering, Technology & Applied Science Research*, vol. 14, no. 1, pp. 12759–12768, Feb. 2024, https://doi.org/10.48084/etasr.6472.

[15] J. Wang, M. Schmitz, L. J. Jacobs, and J. Qu, "Deep learning-assisted locating and sizing of a coating delamination using ultrasonic guided waves," *Ultrasonics*, vol. 141, July 2024, Art. no. 107351, https://doi.org/10.1016/j.ultras.2024.107351.

[16] L. Lomazzi, R. Junges, M. Giglio, and F. Cadini, "Unsupervised data-driven method for damage localization using guided waves," *Mechanical Systems and Signal Processing*, vol. 208, Feb. 2024, Art. no. 111038, https://doi.org/10.1016/j.ymssp.2023.111038.

[17] C. Polle, S. Bosse, and A. S. Herrmann, "Damage Location Determination with Data Augmentation of Guided Ultrasonic Wave Features and Explainable Neural Network Approach for Integrated Sensor Systems," *Computers*, vol. 13, no. 2, Jan. 2024, https://doi.org/10.3390/computers13020032.

[18] D. Mikhaylov, T. Polonelli, and M. Magno, "On-Sensor TinyML Event-Based Fault Detection Strategies on Wind Turbine Blades," in *2024 IEEE Sensors Applications Symposium (SAS)*, Naples, Italy, July 2024, pp. 1–6, https://doi.org/10.1109/SAS60918.2024.10636542.

[19] G. Donati, F. Zonzini, and L. D. Marchi, "Tiny Deep Learning Architectures Enabling Sensor-Near Acoustic Data Processing and Defect Localization," *Computers*, vol. 12, no. 7, June 2023, https://doi.org/10.3390/computers12070129.

[20] V. Nerlikar, O. Mesnil, R. Miorelli, and O. D'Almeida, "Damage detection with ultrasonic guided waves using machine learning and aggregated baselines," *Structural Health Monitoring*, vol. 23, no. 1, pp. 443–462, Jan. 2024, https://doi.org/10.1177/14759217231169719.

[21] X. Wu, M. Wang, J. Lin, and Z. Wang, "Amoeba: An Efficient and Flexible FPGA-Based Accelerator for Arbitrary-Kernel CNNs," *IEEE Transactions on Very Large Scale Integration (VLSI) Systems*, vol. 32, no. 6, pp. 1086–1099, June 2024, https://doi.org/10.1109/TVLSI.2024.3383871.

[22] H. Zhang *et al.*, "Transformer model combining cross-attention and self-attention guided by damage index for pipeline damage localization based on helical guided waves," *Mechanical Systems and Signal Processing*, vol. 231, May 2025, Art. no. 112669, https://doi.org/10.1016/j.ymssp.2025.112669.

[23] J. Moll *et al.*, "Open Guided Waves: online platform for ultrasonic guided wave measurements," *Structural Health Monitoring*, vol. 18, no. 5–6, pp. 1903–1914, Nov. 2019, https://doi.org/10.1177/1475921718817169.